Bedforms induced by solitary waves in a resonator

F. Marin[(1,*)], N. Abcha[(1)], J. Brossard[(1)] and A.B. Ezersky[(2)]

(1) Université du Havre, Laboratoire de Mécanique, Physique et Géosciences, Place R. Schuman, B.P. 4006, 76610 Le Havre, France
(2) Institute of Applied Physics, Russian Academy of Science, 46 Ulyanov Street, 603950 Nizny Novogorod, Russia

Abstract

Experiments on bedforms generation beneath solitary waves have been carried out in a 10 m long resonator. Solitary waves are generated in shallow water against the background of a harmonic wave (Ezersky et al., 2003). One solitary wave (soliton) propagates in each direction of the flume on the time period of the flow. The instantaneous free surface elevation is measured with resistive probes. Fluid velocity measurements are carried out above a flat bed with a two-component laser-Doppler anemometer. Present tests show that nonlinear effects in surface waves significantly affect the bedforms. In particular, the bed remains flat under the antinodes of surface elevation of the standing wave and bars form with crests beneath the nodes of this surface elevation in the suspended load regime.

1. Introduction

The formation of bars beneath standing waves has been widely studied (see, e.g., O'Hare and Davies, 1990). In particular, it is well known that bars wavelength satisfies the Bragg condition with bars spacing equal to half the surface wavelength. Ripples formation under progressive waves in shallow water has also been the subject of numerous studies (Marin et al., 2003). These small scale bedforms have a typical wavelength of about 10 cm. However, very few studies have analyzed the interaction between highly nonlinear waves, such as solitary waves, and a sandy bed. The aim of the present work is to study bedforms generation under solitary waves in a resonator. Solitary waves can be obtained in shallow water in a resonator against the background of a harmonic wave (Ezersky et al., 2003). These solitary waves which can pass through each other and preserve their shape after the collision are often called solitons.

2. Experimental set up

The tests have been carried out in a resonator, a wave flume without absorbing beach, 10 m long and 0.49 m wide. The mean water depth was d = 0.26 m. Surface waves are produced by an oscillating paddle at one end of the flume (Fig. 1). A near perfect reflection takes place at the other end of the flume. The instantaneous free surface elevation is measured with two resistive probes. One probe is located at the reflective end of the flume and the other probe can be moved along the flume. For each test, the wave frequency has been chosen very close to the resonant frequency f_r = 0.165 Hz corresponding to the mode for which the wave length is the flume length. In no test did wave breaking occur in the flume.

* Corresponding author. E-mail: francois.marin@univ-lehavre.fr. Fax: +33 2 32 74 46 71

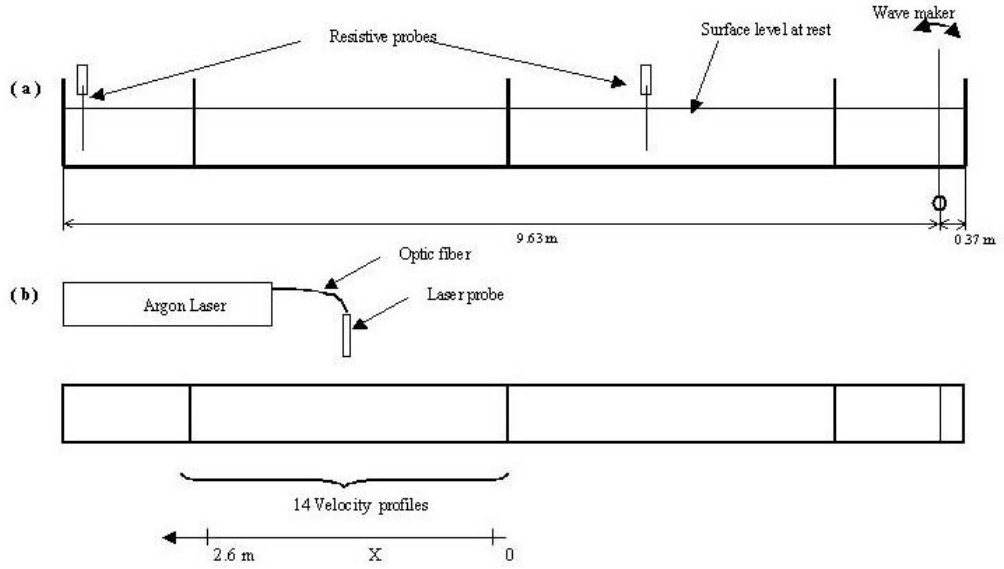

Fig. 1 - Side and top view of the flume

The fluid velocities have been measured in the case where no sediment was introduced in the resonator. These measurements have been carried out with a two-component, 4 W argon laser-Doppler anemometer in backward scatter mode. The measurement volume was 0.14 mm^3. Fourteen vertical velocity profiles were carried out along the channel (Fig. 1), from the bed up to approximately $y = 18cm$, where y is the distance from the bed measured in the vertical direction. The distance between two vertical profiles was 20 cm.

The sediments used consisted of sand characterized by a median grain diameter D_{50} = 0.15 mm and by a relative density s = 2.65. The bed is initially flat. The wave generator is switched on and the redistribution of sand along the channel is analyzed until a stable configuration is reached. Several days may be needed to obtain a stable regime. The temporal evolution of the free surface elevation is regularly recorded.

3. Bars formation induced by standing waves

It is well known that two waves having the same height and period but propagating in opposite directions lead to a standing wave as depicted in Fig. 2. The fluid particles oscillate in a horizontal

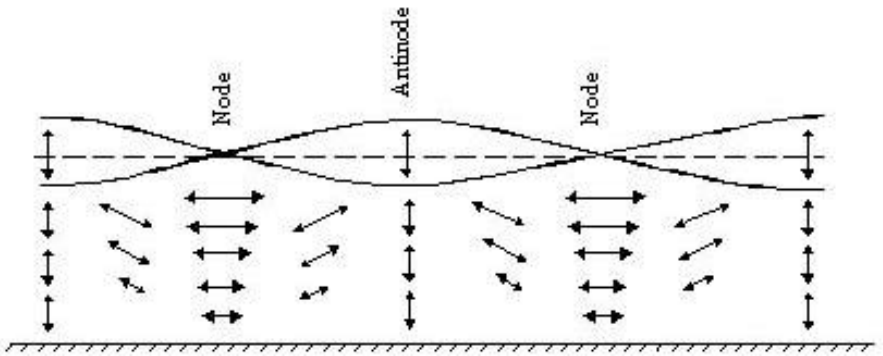

Fig. 2 - Standing wave particle motion and surface profile envelope

plane under a nodal point and in a vertical plane under an antinodal point. Longuet-Higgins (1953) showed theoretically that the steady drift for standing waves takes the form of closed recirculating cells with boundaries at a spacing of one-quarter the wavelength of the surface waves. This is illustrated in Fig. 3 where δ_i is the inner boundary layer thickness. Very close to the bed the fluid

particles drift is oriented towards the nodes of the water surface profile and away from the antinodes. However, the drift is in the opposite direction further out. These recirculating cells generate sediment transport pattern resulting in bar formation, as shown by Nielsen (1979). The bar crests form beneath the antinodes of surface elevation and the bar troughs beneath the nodes when the sediment transport is dominated by the suspensions, the bar wavelength satisfying the Bragg condition.

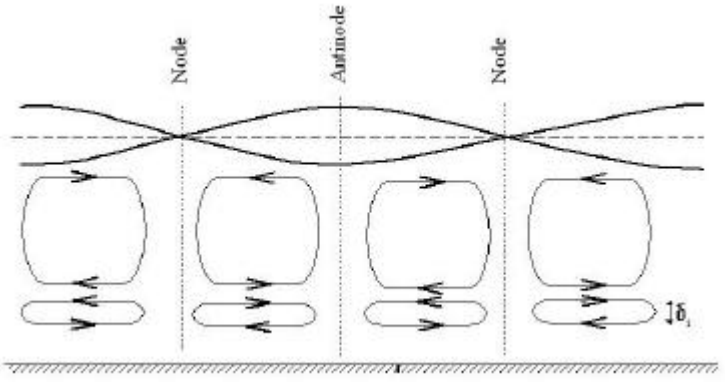

Fig. 3 - Steady drift for standing waves

In the present study, solitary waves are excited on the background of standing waves. Let us consider the bedforms generated in this case.

4. Bedforms induced by solitary waves in the resonator

Preliminary tests carried out without sediments allowed to specify the areas, in terms of frequency and amplitude of the wave paddle movement, of solitary waves excitation (Ezersky et al., 2003). In order to have one solitary wave (one soliton) propagating in each direction of the flume on the time period of the flow, the frequency of excitation was $f = 0.173$ Hz and the amplitude of horizontal displacement of the wave maker averaged over depth was $a_h = 6$ cm, for the test carried out with sediments. Fig. 4 depicts schematically the free surface elevation when the solitons are close to the ends of the flume. Let us consider that they are travelling towards the middle of the channel. The solitons will collide in the central part of the channel, continue their propagation in the same direction until they reach the ends of the flume where they will be reflected. The soliton profiles are well fitted (Ezersky et al., 2003) by the theoretical sech-squared profile:

$$\eta = a_s \operatorname{sech}^2\left[\sqrt{\frac{3a_s}{4d^3}}(x - Vt)\right], \qquad (1)$$

where η is the free surface elevation, a_s the amplitude of soliton, d the water depth at rest, V the propagation velocity of soliton and t the time.

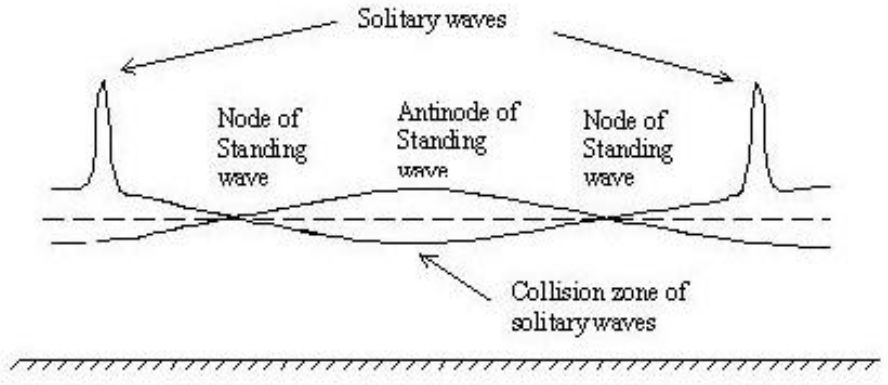

Fig. 4 - Schematic surface profile when the solitons are close to the flume ends

At the beginning of the test, the bed was flat and a 20 mm sand layer recovered the bottom. Fig. 5a shows schematically the initial sand distribution along the channel (t = 0), and Fig. 5b the temporal evolution of the free surface at the reflective end of the flume (t = 3 mn40), where the level 0 mm corresponds to the water level at rest. Small ripples form rapidly after a few minutes of surface waves excitation. These ripples spread all-over the flume length, except in the middle part where the bed remains flat along approximately 40 cm. This middle part corresponds to the region of collision of the two contra-progressive solitary waves which move from one end of the flume to the other. The fluid velocities are very small near the bed in this area; the value of the bed shear stress is below the critical value for the initiation of movement of sand and the bed is not affected by the surface waves in the central part of the flume. In the other parts, the ripple size progressively increases and a strong interaction with the free surface occurs. Fig. 5c and 5d depict respectively the distribution of sand along the channel and the temporal evolution of the free surface at t = 30 mn, that is after approximately 310 excitation cycles. The peak value of the surface elevation is significantly lower than the corresponding value at t = 0 due to dissipation at the bed boundary layer, and the width of this peak is larger than at t = 0. The increase of the peak width for a decreasing value of the peak value is a typical property of solitons (Remoissenet, 1996). At a given time, the ripple size depends on the local orbital amplitude of fluid; starting from the flat bed in the central part of the channel, ripple length and height progressively increase with distance x along the wave flume (in both directions). The ripple size is maximal at about 2 m from the flume centre; beyond this area, the ripple size decreases for increasing values of x.

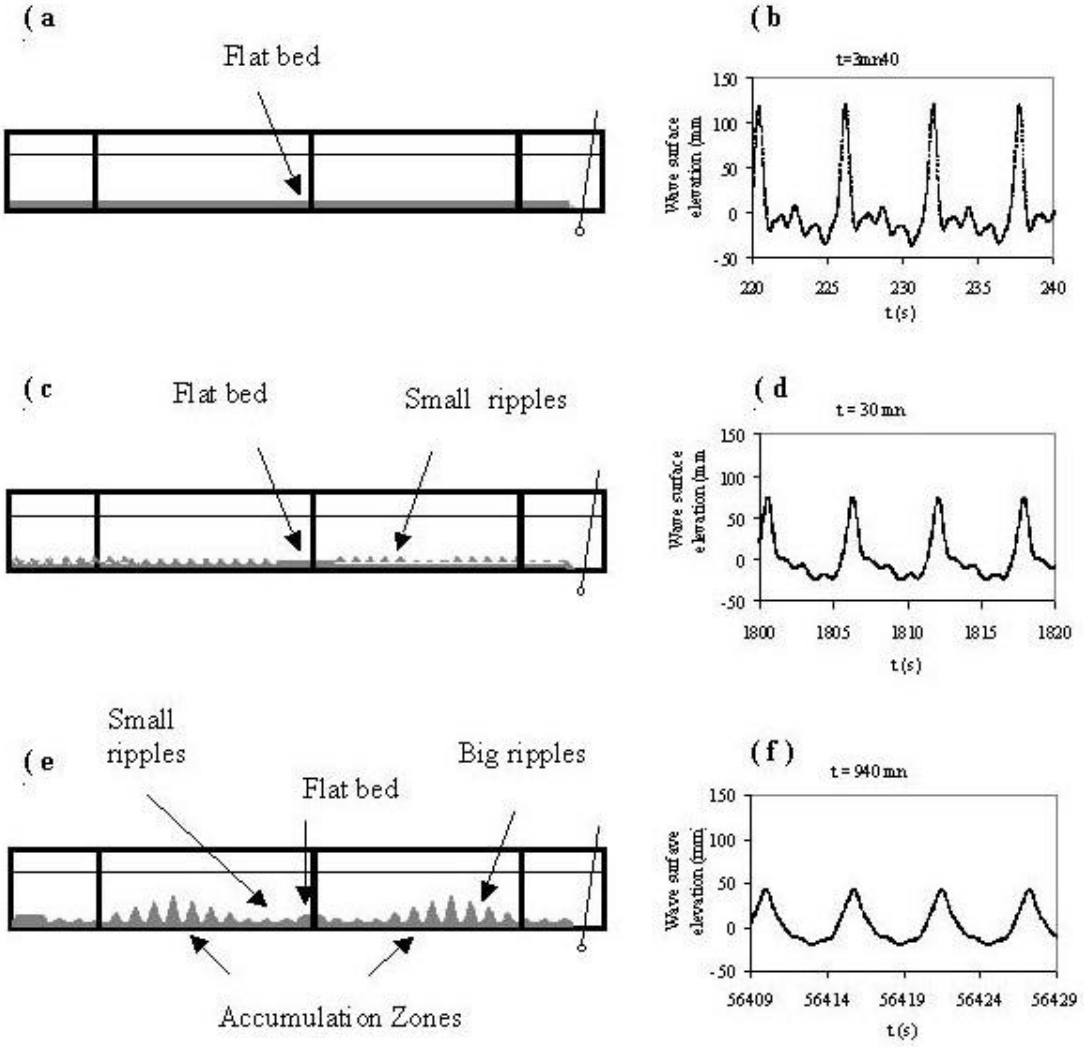

Fig. 5 - Schemes of sand distribution in the flume (a,c,e) and temporal evolution of the free surface (b,d,f); (a,b): Beginning of the test, (c,d): t = 30 mn, (e,f): t = 940 mn

The dynamics of bed evolution is then slower. At t = 940 min, that is after about 9760 excitation cycles, two sand accumulation zones have clearly appeared, as shown in Fig. 5e. These zones are symmetrical in respect to the vertical plane oriented perpendicularly to the longitudinal axis of the flume and crossing the flume centre (x = 0). The accumulation zones progressively develop and form bars with crests located beneath the nodes of surface elevation. As mentioned in section 3, bar crests position beneath the antinodes of surface elevation in the case of standing waves. This is an important difference with present tests involving solitary waves in a resonator, as it was shown in the case of partially-standing waves by O'Hare and Davies (1990), that the bar position is a very significant parameter as far as the ability of bars to reflect incident wave energy is concerned. This may have significant practical application as it is well known that as a long period oscillatory wave propagates in very shallow water of decreasing depth, the surface profile approaches the solitary wave form before waves breaking. The largest ripples establish in the vicinity of bar crests where the ripple wavelength and height are approximately 15 cm and 4 cm, respectively. Fig. 6 shows a series of four photographs which have been assembled to depict the sand distribution along 6 m in the central part of the flume after approximately 4800 minutes of surface waves excitation.

Fig. 6 - Sand distribution induced by solitary waves along 6 m of the flume (central part)

5. Eulerian drift beneath solitary waves in the resonator

In order to improve the understanding of the distribution of sediments beneath solitary waves in the resonator, fluid velocities were measured without sand at the bottom, with the same flow conditions as the test carried out with sand (d = 0.26 m; f = 0.173 Hz; a_h = 6 cm). Vertical velocity profiles have been carried out along 2.60 m of the flume (Fig. 1). At each measurement point, data acquisition was performed during 180 s with an acquisition frequency of 50 Hz. Fig. 7 presents the temporal evolution of the horizontal and vertical components of velocity (u and v, respectively), at 0.80 m downwards from the flume centre and at 95 mm from the bottom. The velocity peaks correspond to the passage of solitons.

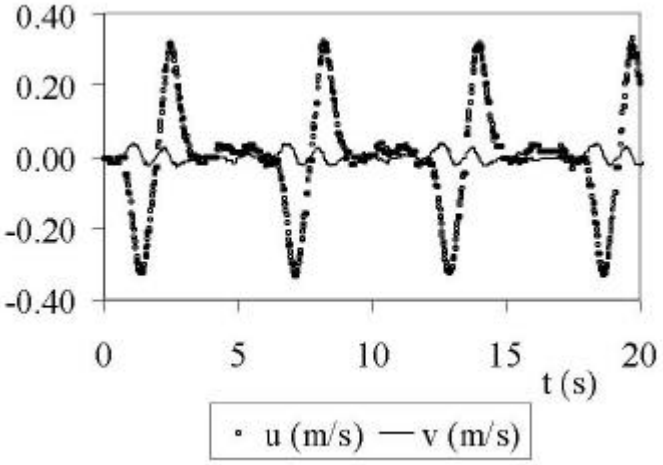

Fig. 7-Temporal evolution of the horizontal and vertical components of velocity (x=0.80 m; y=95 mm)

Let us consider the Eulerian drift in the resonator, that is the velocity time-mean values at fixed measurement points. Fig. 8 shows the distribution of time-mean velocity vectors. A clockwise recirculating cell can clearly be seen in the upper part of the flow. Present tests involving high velocities induced a lot of sand suspension. For y > 10 cm, the drift velocities are oriented towards the node of surface elevation of the standing wave ($x \approx 2.40$ m) when x > 0 (downwards the central antinode of surface elevation) and x < 1.50 m. For higher values of x, that is at greater distances from the wave paddle, high vertical velocities oriented towards the bottom take place. This distribution of

Eulerian drift may have a significant effect on the final distribution of sediments, bar crests being located approximately beneath the nodes of surface elevation. Let us now focus our attention on the steady streaming close to the bed where vertical drift velocities are negligible.

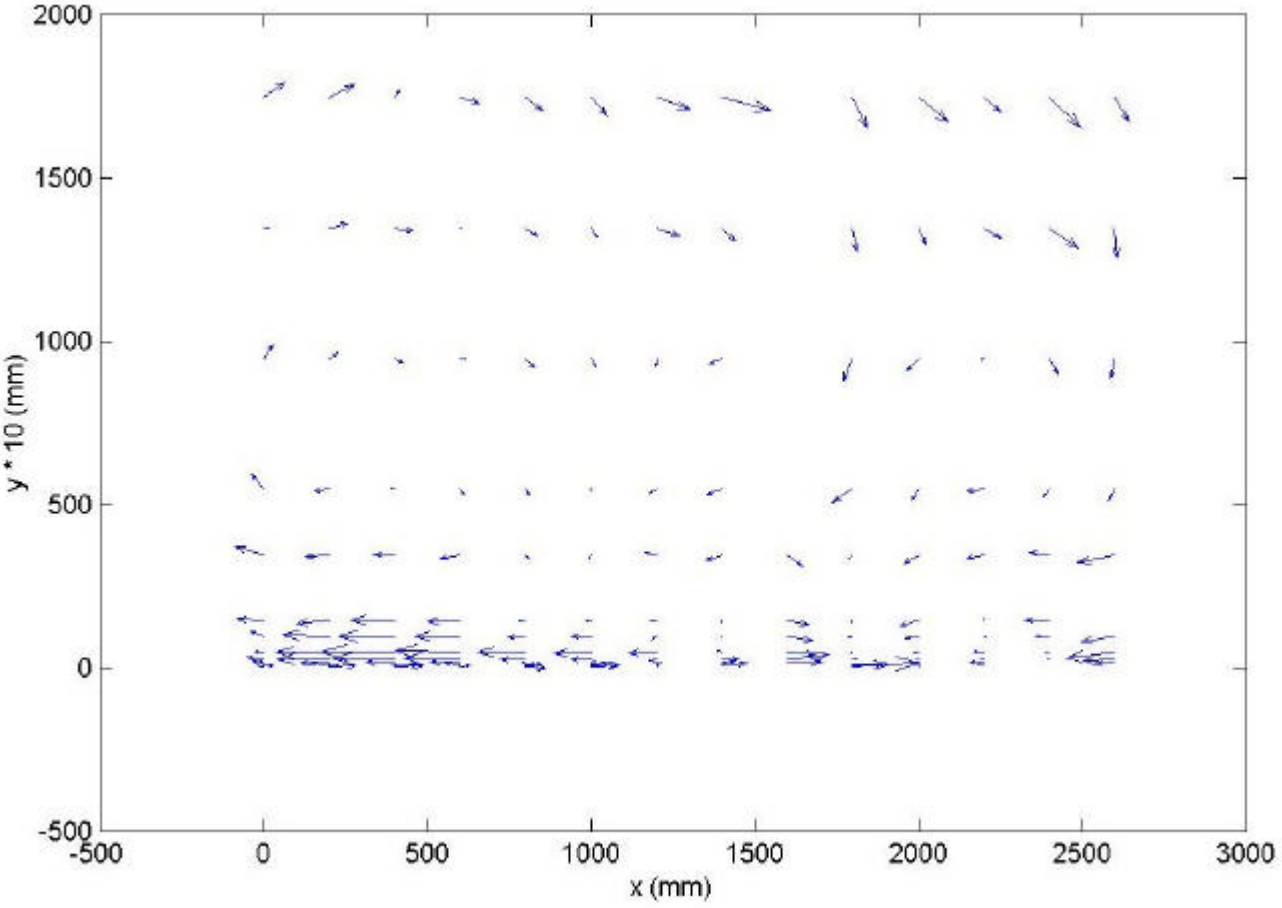

Fig. 8 - Distribution of time-mean velocity vectors; $\longrightarrow$ 0.007 m s^{-1}

Fig. 9 presents the vertical profiles of $\bar{u}$, the horizontal component of Eulerian drift, for y < 15 mm. In the central part of the flume (x = 0), the drift velocity is close to zero in the vicinity of the bed. For $x = 800$ mm, the drift velocity is positive, that is oriented towards the reflective fixed wall of the channel, for y < 1.5 mm. The drift velocity is oriented in the opposite direction for greater values of y, that is outside the Stokes boundary layer thickness δ_i ($\delta_i = \sqrt{\nu T/\pi} = 1.4$ mm). Fig. 9 shows that for $x > 2200$ mm, the drift velocity reverses close to the bottom and orientates towards the wave maker. Let us focus on the profile at x = 2600 mm. There is no change in the steady streaming direction just outside the Stokes boundary layer and the drift is towards the wave maker up to approximately half the water level at rest (Fig.8). The bar crests observed in the present study are positioned at the convergence area of the drift velocity vectors in the Stokes boundary layer, approximately beneath the nodes of surface elevation. The bed remains flat beneath the antinode of surface elevation in the central part of the flume. In the case of purely standing waves, the bars form with crests beneath the antinodes of surface elevation, at the convergence area of the drift velocity vectors just outside the Stokes boundary layer.

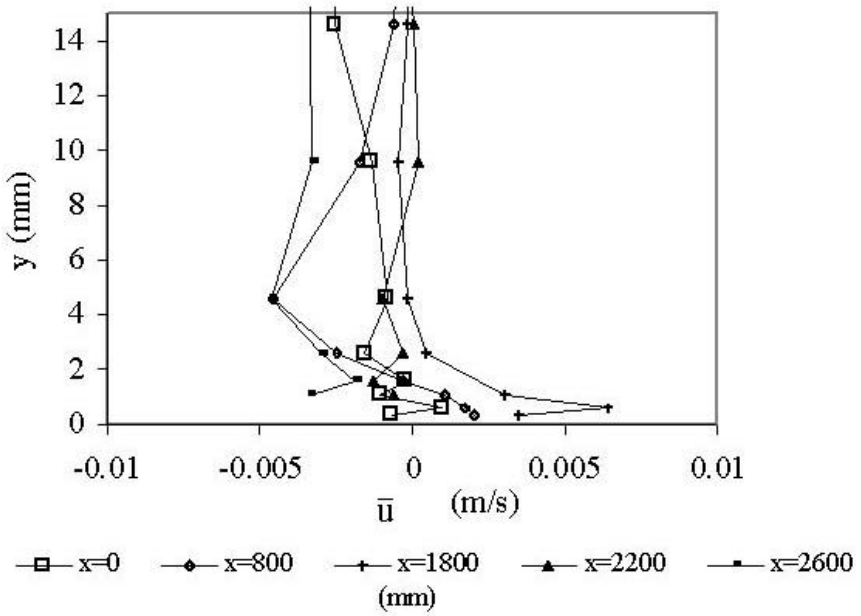

Fig. 9 - Vertical profiles of the drift velocity $\bar{u}$

6. Conclusion

Experiments have been carried out on bedforms induced by solitary waves (solitons) in a resonator. The profiles of soliton generated in the resonator are well fitted by the theoretical sech-squared profile (Ezersky et al., 2003). One solitary wave propagated in each direction of the flume on the time period of the flow above an initially flat sand bed. The experiments show that nonlinear effects in surface waves significantly affect the bedforms. In particular, the bed remains flat under the antinodes of surface elevation of the standing wave and bars form with crests beneath the nodes of this surface elevation. This may have practical application in the ability of bars to reflect incident wave energy in the case of long period oscillatory waves propagating in very shallow water of decreasing depth. The Eulerian drift velocities which have been measured with a two-component laser-Doppler anemometer may explain the final distribution of sand.

References

A.B. Ezersky, O.E. Poloukhina, J. Brossard, F. Marin and I. Mutabazi, Modelisation des ondes solitaires excitees dans un canal en eau peu profonde, *16eme Congres Francais de Mecanique, Nice, 1-5 septembre 2003 (on CD).*

M.S. Longuet-Higgins, Mass transport in water waves, *Philos. Trans. R. Soc. Lond.,* A 245 (903), pp. 535-581, 1953.

F. Marin, A. Jarno-Druaux and J. Brossard, Formation dynamics and geometry of ripples under waves, *in: E.Foti, J. Fredsøe (Eds), Sea Wave Bottom Boundary Layer, Euromech Colloquium 451,Taormina, Italy, October, 26-29 2003*, pp. 75-76, 2003.

P. Nielsen, Some basic concepts of wave sediment transport. *Institute of Hydrodynamics and Hydraulic Engineering,* Series Paper N°20, 160 p., 1979.

M. Remoissenet, Waves called solitons: Concepts and Experiments. Springer-Verlag, Berlin, 1996.

T. J. O'Hare and A.G. Davies, A laboratory study of sand bar evolution, *J. of Coastal Res.*, Vol. 6(3), pp. 531-544, 1990.